The pH Effect on the Preparation of MFI Type Ferrisilicate Zeolites

Young-Hoon Yeom, Sang-Sung Nam, Seong-Bo Kim, and Kyu-Wan Lee*

Chemical Technology Division I, Korea Research Institute of Chemical Technology, Taejon 305-600, Korea
Received May 28, 1999

Ferrisilicates with MFI type structure were hydrothermally synthesized. The structural environments of iron in the ferrisilicates were characterized by XRD, SEM, IR, EPR, and ammonia-TPD. It has been shown that pH of the final gel mixture during the synthesis affects the crystal size, morphology, chemical composition and catalytic activity. The results of the lattice parameters, IR, and EPR indicate the existence of a framework iron and the content of framework iron depends on pH of the synthesis gel. Finally, the catalytic activity of these zeolites was examined for the cyclohexane oxidation to cyclohexanol and cyclohexanone in the liquid phase. The conversion of this reaction was increased with increasing iron content of the framework lattice positions.

Introduction

With the growing interest in the usage of zeolites as catalysts, more attention has been paid to the modification of zeolite properties by incorporating transition metals into the zeolite framework. This modification is aimed at bringing about changes in the chemical and physical properties and to induce new catalytic properties maintaining the original crystal structure of the zeolite. Subsequently, various metal elements such as Co,[1] Cu,[2] Mn,[3] Ni,[4] Sn,[5] Ti,[6] V,[7] Zn,[8] and Zr[9] were incorporated into the zeolite framework.

Iron cation can be incorporated into the tetrahedral framework sites of a molecular sieve structure during the ferrisilicate synthesis. The degree of iron substitution is generally very low. However, the amount of iron incorporated is dependent on the synthetic conditions.[10,11] Iron does not necessarily occupy exclusively the framework sites of ferrisilicates. It can also exist in the ion exchange sites as the charge balancing cations and also in the ferrisilicate cavities as the small iron oxide particles.[2,12-14] Some of the techniques such as Mössbauer,[12,15,16] EPR,[2,17,18] and EXAFS[19,20] are commonly used to characterize these iron sites.

Szostak *et al.*[10,11] prepared ferrisilicate with MFI structure from ferrisilicate gels containing low-molecular-weight silica species. In this study, they suggested that the acidic pH of the solution containing Fe^{3+} ion is critical in the successful preparation of MFI ferrisilicate. They discussed that the initial formation of a ferrisilicate complex at low pH avoids precipitation of rust-red iron hydroxide and once iron is complexed in this manner, the formation of ferric hydroxide at elevated pH appears to be suppressed. However, we confirmed that the ferrisilicate complex formed is not stable under the synthesis conditions and the content of the framework incorporated iron is mostly depend on the final pH of the final synthesis gel.

In this paper, the MFI type ferrisilicates were hydrothermally synthesized under the different pH of the final synthesis gel and the relation between the content of the framework incorporated iron and the pH effect was examined. The framework incorporation of iron has been studied by lattice parameters, IR, EPR, and TPD techniques. Finally, catalytic activity over these catalysts was examined for cyclohexane oxidation to cyclohexanol and cyclohexanone with hydrogen peroxide.

Experimental

MFI type ferrisilicate (Si/Fe = 300) molecular sieves were hydrothermally synthesized at autogeneous pressure. In a typical preparation, 0.91 g of $Fe(NO_3)_3 \cdot 9H_2O$ (98% Aldrich) was dissolved in a solution containing 60 g of H_2O and 1.0 g of H_2SO_4 (96%), and 42.5 g tetraethylorthosilicate (TEOS) (98% Aldrich) were added slowly to this clear solution under vigorous stirring. The resulting yellow solution was stirred at 298 K for 3 h. To the above gel, 25.5 mL of tetrapropylammonium hydroxide (TPAOH) (1.0 M in methanol, Aldrich) as a template was added. Finally, the required amount of NaOH dissolved in 100 g of H_2O was added to the above mixture under vigorous stirring to adjust pH of the gel. The pH of this gel was measured at 25 °C with a plastic-bodied combination pH electrode in conjunction with a digital pH meter (ORION, model 420A). The resulting white gel was transferred to a Teflon lined stainless-steel autoclave and heated at 443 K for 5 days. The resulting product was washed several times and calcined with a 2-step calcination. First these samples were calcined under nitrogen flow at 773 K for 8 h followed by air flow at 773 K for 4 h. For ammonia-temperature programmed desorption (TPD) study, the calcined samples were ion-exchanged four times in NH_4OH solution (0.5 N) at 25 °C for 3 h followed by calcination at the same condition to obtain the hydrogen form of ferrisilicates. Ferrisilicates prepared at different pH will be hereinafter denoted as FeS1-1 (pH = 8), FeS1-2 (pH = 9), FeS1-3 (pH = 10), and FeS1-4 (pH = 11), respectively.

Characterization

Powder X-ray diffraction (XRD) patterns of these pre-

pared samples were recorded using a Rigaku D/max-B X-ray diffractometer with nickel filtered CuK_α radiation (λ = 1.5406 Å). Scanning electron microscopes were obtained in a JEOL JSM-840A microscope operating at 20 KV. FT-IR measurements were done with KBr-pressed wafers on Digilab FTS-165 spectrometer. Electron paramagnetic resonance spectra was recorded on Bruker ESP-300 spectrometer at liquid nitrogen temperature. Acidity measurements were determined by ammonia-TPD by using a conventional flow system with a thermal conductivity detector. About 0.5 g of sample was loaded in a quartz reactor and heated at 873 K for 4 h under argon atmosphere. After cooling the sample to 373 K, pure ammonia was adsorbed for 1 h. Then the sample was swept with helium for 30 min at 373 K to remove physisorbed ammonia and finally, TPD measurement was performed from 373 to 873 K at a heating rate of 3 K/min.

The catalytic activity for cyclohexane oxidation was tested in a Teflon-lined 450 mL Parr autoclave equipped with a mechanical stirrer. The ratio of acetone (Mallinckrodt, 99.6%)/cyclohexane (Merck, 99.5%)/H_2O_2 (30% soln., Junsei) was 30/4/4 (v/v/v) giving a total of 38 mL; 0.20 g of catalyst. The autoclave was closed and maintained at 343 K for 4 h. After the reaction, the products were analyzed by gas chromatograph (Shimadzu GC-8A).

Results and Discussion

XRD. The X-ray diffraction patterns of calcined ferrisilicates are shown in Figure 1. The symmetry of the calcined FeS1 zeolites is orthorhombic.[21] In the calcined silicalite-1 crystals with a monoclinic symmetry, the splitting of reflections in the XRD pattern is usually observed at 2θ = 24.4° and 29.3° (Figure 1(a)).[22,23] Therefore, the persistence of the orthorhombic symmetry even in the calcined state provides supplementary evidence for the lattice positions of iron in the ferrisilicates.[22,23]

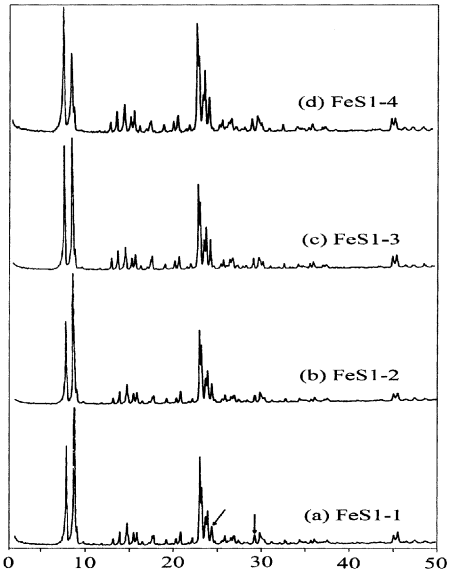

Figure 1. X-ray powder patterns of MFI-type ferrisilicates calcined at 500 °C.

Table 1. Crystal data for MFI-type ferrisilicates

ferrisilicates	a (Å)	b (Å)	c (Å)	V ($Å^3$)
FeS1-1	20.149	19.958	13.430	5400.5
FeS1-2	20.100	19.925	13.405	5368.4
FeS1-3	20.089	19.916	13.396	5360.0
FeS1-4	20.082	19.909	13.395	5355.6

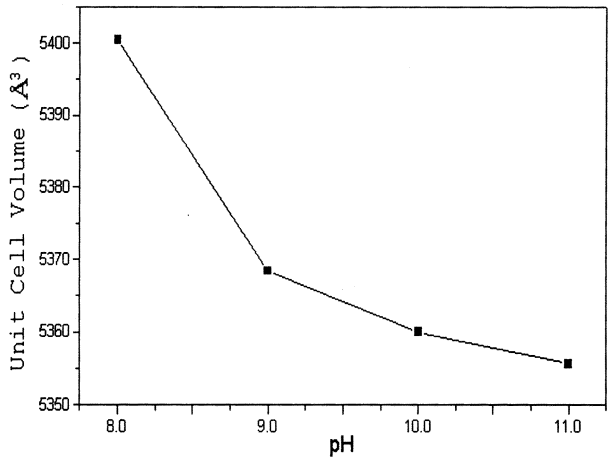

Figure 2. The unit cell volume *vs* pH of the synthesis gel of MFI-type ferrisilicates calcined at 500 °C.

The unit cell parameters of FeS1 were obtained by least-square fit to interplanar spacings of selected reflections in the X-ray diffraction pattern. The unit cell parameters are listed in Table 1. The replacement of Si by the larger iron in the tetrahedral zeolite framework causes a slight expansion in the unit cell parameters due to the difference in the bond lengths between Si-O (1.61 Å) and Fe-O (1.88 Å). The unit cell volumes are plotted against pH of the final synthesis gel (Figure 2). Each of FeS1 does not have an identical volume. It is clear that this is due to the difference of the lattice iron content. This indicates that the incorporated iron content depends on the pH of the final synthesis gel.

Morphology. The scanning electron micrographs of four crystalline products are shown in Figure 3. Each of four samples has almost monodisperse size distributions. When the pH of the gel mixtures is maintained at 9, regular twinned and elongated crystals are formed with a size about 30 μm in length. Small cube-shape crystals of 2 μm were obtained when the pH of the gel mixtures was increased to 11. It is well known that more nuclei are formed in the higher alkalinities in the synthesis MFI type silicalite-1.[24] Therefore, the crystal size of ferrisilicates decreases with increasing the pH of the synthesis gel.

FT-IR. Infrared spectroscopy provides supplementary evidence for framework incorporation of iron. In all zeolites, symmetric and asymmetric stretching vibrations of the (Si O Si(Al))$_n$ group generally appear between 600 and 1250 cm^{-1}.[25] The FT-IR spectra for four samples are shown in Figure 4. The broad absorption bands have appeared at 960 cm^{-1} and 1060 cm^{-1} in samples (a)-(c). It is well known that the absorption bands at these regions are due to the

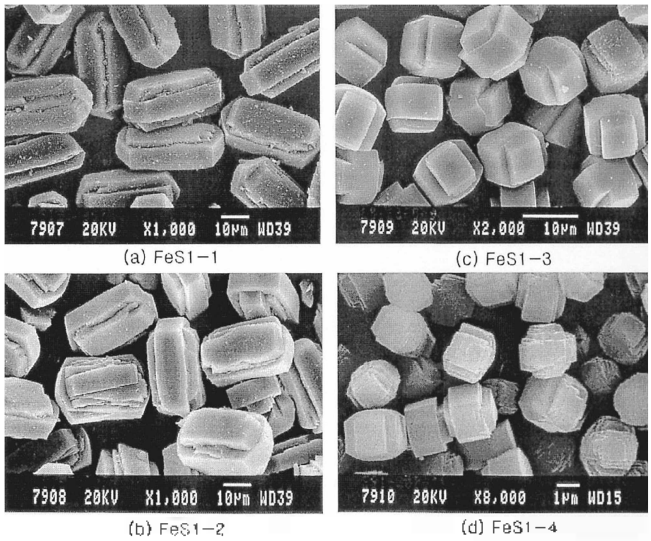

Figure 3. Scanning electron micrographs of calcined MFI-type ferrisilicates.

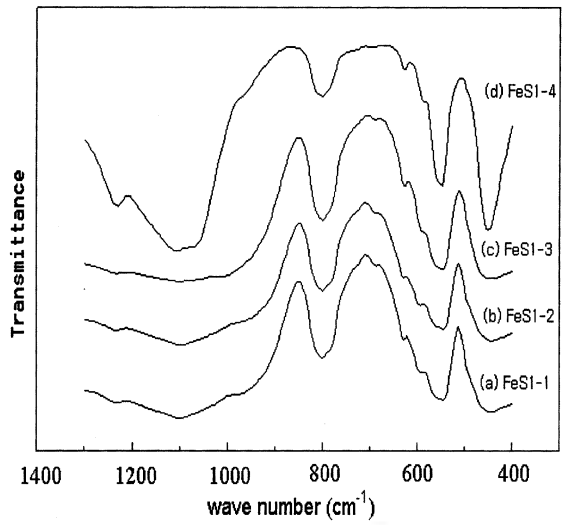

Figure 4. FT-IR spectra of MFI-type ferrisilicates calcined at 500 °C.

(Si O Fe)$_n$ asymmetric vibration of iron incorporated zeolites with MFI type topology.[11,26] These are not observed in the calcined silicalite-1.[11,26,27] Although there are no marked differences between the spectra in samples (a)-(c), these broad bands are due to incorporated iron in the tetrahedral framework. The band broadening at 960 cm^{-1} and 1060 cm^{-1} for sample (d) is significantly decreased comparing to three samples (a)-(c). This indicates that the content of incorporated iron is very low in sample (d). This observation is in agreement with the results of crystal data.

EPR measurements. The EPR spectra of the crystalline iron-containing samples are shown in Figure 5. The broad signal at $g = 2$ and sharp signal at $g = 4.3$ are the major. Similar spectra were reported previously in other works.[2,15,17,18,28,29] Generally the former is attributed to nonframework hexacoordinate Fe^{3+}, the latter is assigned to tetrahedral Fe^{3+} possibly in lattice positions.[17,30] With increasing the pH of the synthesis gel, the intensity of the EPR signal for tetrahedral iron can be seen to decrease in Figure 5 (a)-(d). Therefore, we can conclude that the content of framework iron is increased with decreasing the pH of the final synthesis gel. This interpretation is consistent with the crystal data and FT-IR results.

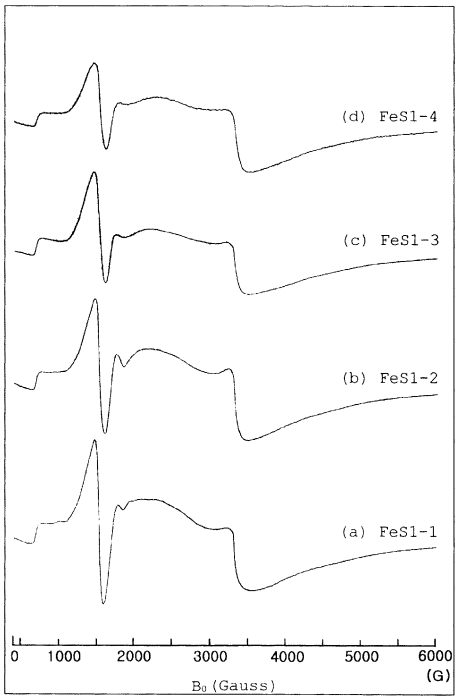

Figure 5. Electron paramagnetic resonance spectra of MFI-type ferrisilicates measured at liquid nitrogen temperature.

The intense peak at $g = 2.0$ arises from iron in hydroxide phases and cation exchange sites.[17,30] This indicates that a large proportion of the iron exists as nonframework iron species in calcined ferrisilicate. It is reported that iron-oxygen clusters (*i.e.* $[Fe(H_2O)_6]^{3+}$, various hydrolysis products $[Fe(H_2O)_n(OH)_{6-n}]^{(3-n)+}$, and multinuclear Fe^{III} complexes) give a strong and broad resonance at about $g = 2$.[30]

Temperature Programmed Desorption. The number

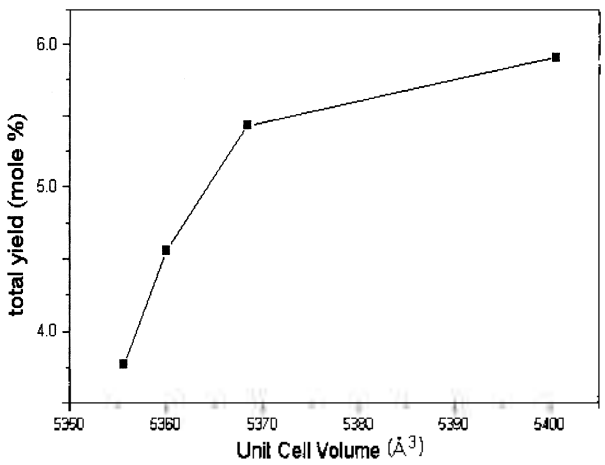

Figure 6. The relation between the unit cell volume and the total yield (cyclohexanol + cyclohexanone) of cyclohexane oxidation.

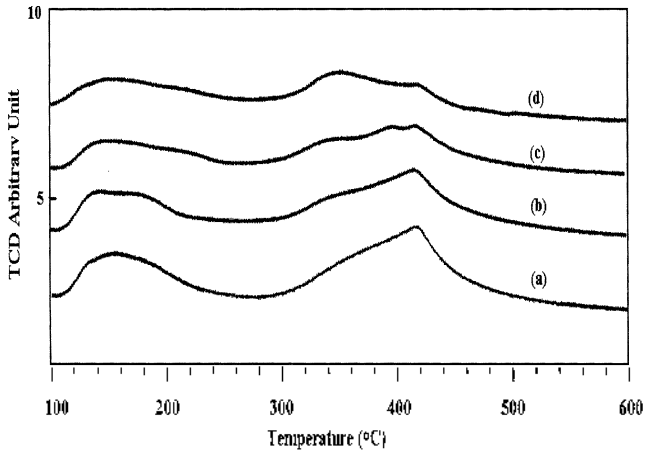

Figure 7. Comparison of NH3-TPD profiles of ferrisilicates. (a) H-FeS1-1. (b) H-FeS1-2. (c) H-FeS1-3. (d) H-FeS1-4

of acid sites and the distribution of acid strength of FeS1 samples can be surmised from the TPD spectra. Figure 7 shows the ammonia-TPD profiles of Fe-silicates. Two peaks, at about 150 and 420 °C indicating the presence of weak and strong acid sites in appreciable portions. It increases the number of strong acid site and weak acid site as follows: H-FeS1-1 > H-FeS1-2 > H-FeS1-3 H-FeS1-4. Therefore, the number of both acid sites gradually increases with increasing the content of iron cation in the framework position.

Activity test. Finally, these samples were used as a catalysts on the oxidation of cyclohexane to cyclohexanol and cyclohexanon in the presence of H_2O_2. The results were shown in Table 2 and the total yield against the unit cell volume was plotted in Figure 6. It can be seen that the catalytic activity of ferrisilicate samples in the cyclohexane oxidation increases with increasing the unit cell volume. This indicates that the highly dispersed iron species incorporated in the framework sites are mainly responsible for the active species in the cyclohexane oxidation.

The pH effect on the framework incorporation of iron. To optimize the synthesis of ferrisilicates, the following procedures are adopted in the synthesis steps: (1) TEOS with neutral pH as silica source is used to avoid the precipitation of iron as rust-red iron hydroxides, (2) TEOS solution is hydrolyzed in the acidic condition with sulfuric acid and iron(III) nitrate solution is added to the above gel to avoid the precipitation of iron during the gel forming with silica,

Table 2. The result of catalytic activity test of MFI-type ferrisilicates for cyclohexane oxidation

catalysts	cyclohexanol (mole %)	cyclohexanone (mole %)	total (mole %)	-one/-ol
FeS1-1	2.81	3.10	5.91	1.10
FeS1-2	2.60	2.83	5.43	1.09
FeS1-3	2.12	2.43	4.55	1.15
FeS1-4	1.71	2.07	3.78	1.21

Reaction conditions: 0.2 g of catalyst, 4 mL of cyclohexane, 30 mL of acetone, 4 mL of H_2O_2 (30% in H_2O), 70 °C of reaction temperature, stirred for 4 h in a Teflon-lined Parr autoclave.

and (3) the pH of the reaction mixture is adjusted to the basic pH with NaOH to control pH of the final synthesis gel and promote crystallization of ferrisilicates.

Although the crystallization is initiated from the reactants with the same SiO_2/Fe_2O_3 ratio in the synthesis gel, the content of framework iron of ferrisilicate is different. This is due to the different synthesis conditions employed, mainly pH of the synthesis gel. The final pH of the synthesis gel has to be adjusted with NaOH to the basic conditions necessary to promote molecular sieve crystallization. However the basic condition has an critical effect on the framework incorporation of iron in ferrisilicate synthesis.

Bellussi *et al.*[31] prepared vanadiumsilicates by varying concentration of NaOH in the gel mixture during the synthesis and suggested the Na^+ ions affects the state of the vanadium contained in the crystalline solid and its stability to the thermal treatments. Dewer *et al.*[32] prepared Al- and Ga-substituted MFI zeolites from a sodium-free system in the presence of fluoride ions. They confirmed that the compositions of the products have the least value for Si/M ratio, when the pH of the synthesis gels is near to neutral. In the case of the synthesis of aluminosilicate zeolites, alumina-rich zeolites crystallize preferably at a higher pH in the mean while silica-rich zeolites crystallize preferably at a lower pH.[33]

Szostak *et al.*[11] suggested that initial ferrisilicate complex in the synthesis had to be prepared under an acidic condition to avoid precipitation of rust-red iron hydroxides and, once iron was complexed in this manner, the formation of ferric hydroxides appeared to be suppressed at elevated pH. In that work, they only focused on the formation of initial ferrisilicate complex and they discussed that the pH for the successful preparation of ferrisilicate was need to be adjusted between 8 and 11 required for the hydrothermal crystallization. However they did not consider a systematic study between the framework iron content and the pH of the final synthesis gel. Moreover, they did not recognize that the pH of the final gel mixture plays a critical role in the framework incorporation of iron.

It is well known that iron tends to precipitate as a rust-red colloidal ferric hydroxides at pH > 4. At elevated pH the decrease of the framework iron content suggests that colloidal iron hydroxides may be formed by dissolution of the greater part of iron from the depolymerization reactions of the ferrisilicate gel formed at the initial synthesis step. On the contrary, at relatively lowered pH the increase of the content of the framework iron suggests that the greater part of iron is present in the highly dispersed form in the ferrisilicate complex and this precursor is responsible for the framework incorporation of iron in the ferrisilicates. But we confirmed that if the pH of the synthesis gel is lowered to 7 and below, they lost their crystallinity after calcination for 5 h at 500 °C. Thus, the optimum pH for the synthesis of the highly incorporated iron ferrisilicates is around 8.

Conclusions

MFI type ferrisilicates are prepared at different pH of the

final synthesis gel. The final pH of the synthesis gel has to be adjusted with NaOH to the basic conditions necessary to promote molecular sieve crystallization. However, the basic pH of the synthesis gel has a critical effects in iron incorporation into a lattice positions. Basic pH causes the partial breaking of ferrisilicate complex by depolymerization reaction and induces the formation of colloidal iron hydroxide phases. Also it had been shown that pH greatly affects the size and morphology of the crystals produced. The coordination state of Fe^{3+} has been investigated by crystal data, IR, EPR and TPD. The incorporation of Fe^{3+} ions in the lattice positions was evidenced by a change in the unit cell parameters and unit cell volume. The broad bands of the IR framework vibration at the regions between 960 cm^{-1} and 1060 cm^{-1} also indicated of the existence of a lattice iron. EPR spectra at $g = 4.3$ corresponds to the presence of tetrahedral iron species and the relative intensity was increased with decreasing the pH of the synthesis gel. The ammonia-TPD result showed the amount of acid sites increased with increasing the content of framework iron. Catalytic activity in the cyclohexane oxidation was increased with increasing the iron content of a lattice positions. This indicated that the incorporated iron in the framework sites was mainly responsible for the active species.

References

1. Xu, H. S.; Pu, S. B.; Inui, T. *Catal. Lett.* **1995**, *35*, 327.
2. Catana, G.; Pelgrims, J.; Schoonheydt, R. A. *Zeolites* **1995**, *15*, 475.
3. Zhao, D.; Goldfarb, D. *J. Chem. Soc. Chem. Commun.* **1995**, 875.
4. Xu, H. S.; Pu, S. B.; Inui, T. *Catal. Lett.* **1996**, *41*, 83.
5. Mal, N. K.; Ramaswamy, V.; Ganapathy, S.; Ramaswamy, A. V. *Appl. Catal. A: General* **1995**, *125*, 233.
6. Duprey, E.; Beaunier, P.; Springuel-Huet, M. A.; Bozon-Verduraz, F.; Fraissard, J.; Mandoli, J. -M.; Breg aui, J. M. *J. Catal.* **1997**, *165*, 22.
7. Hari Prasad Rao, P. R.; Belhekar, A. A.; Hegde, S. G.; Ramaswamy, A. V.; Ratnaswamy, P. *J. Catal.* **1993**, *141*, 595.
8. Röhrig, C.; Gies, H.; Marler, B. *Zeolites* **1994**, *14*, 498.
9. Rakashe, B.; Ramaswamy, V.; Ramaswamy, A. V. *J. Catal.* **1996**, *163*, 501.
10. Szostak, R.; Thomas, T. L. *J. Catal.* **1986**, *100*, 555.
11. Szostak, R.; Nair, V.; Thomas, T. L. *J. Chem. Soc., Faraday Trans. I* **1987**, *83*, 487.
12. Chandwadker, A. J.; Date, S. K.; Bill, E.; Trautwein, A. *Zeolites* **1992**, *12*, 180.
13. Meagher, A.; Nair, V.; Szostak, R. *Zeolites* **1988**, *8*, 3.
14. Derouane, E. G.; Mestsdagh, M.; Vielvoye, L. *J. Catal.* **1974**, *33*, 169.
15. Calis, G.; Frenken, P.; de Boer, E.; Swolfs, A.; Hefni, M. A. *Zeolites* **1987**, *7*, 319.
16. Lázár, K.; Borbély, G.; Beyer, H. *Zeolites* **1991**, *11*, 214.
17. Goldfarb, D.; Bernardo, M.; Strohmaier, K. G.; Vaughan, D. E. W.; Thomann, H. *J. Am. Chem. Soc.* **1994**, *116*, 6344.
18. Joshi, P. N.; Awate, S. V.; Shiralkar, V. P. *J. Phys. Chem.* **1993**, *97*, 9747.
19. Matsubayashi, N.; Shimada, H.; Zmamura, M.; Sato, T.; Okabe, K.; Yoshimura, Y.; Nishijima, A. *Catal. Today* **1996**, *29*, 273.
20. Axon, S. A.; Fox, K. K.; Carr, S. W.; Klinowski, J. *Chem. Phy. Lett.* **1992**, *189*, 1.
21. *Collection of Simulated XRD Powder Patterns for Zeolites;* Treacy, M. M. J.; Higgins, J. B.; Von Ballmoos, R. Eds.; Elsevier: 1996; p 525.
22. (a) Millini, R.; Massara, E. P.; Perego, G.; Bellussi, G. *J. Catal.* **1992**, *137*, 497. (b) Kumar, A. T. R.; Mirajkar, S. P.; Ratnasamy, P. *J. Catal.* **1991**, *130*, 1.
23. Sulikowski, B.; Klinowski, J. *Zeolite Synthesis*; Occelli, M. L.; Robson, H. E. Eds.; American Chemical Society: Washington DC, 1989, chapter 27, p 393.
24. Fegan, S. G.; Lowe, B. M. *J. Chem. Soc., Faraday Trans. I* **1986**, *82*, 785.
25. Breck, D. W. *Zeolite Molecular Sieves: Structure of Zeolites by Infrared Spectroscopy*; John Wiley-Interscience: New York, 1974.
26. Goldwasser, M. R.; Navas, F.; Zurita, M. J. P.; Cubeiro, M. L.; Lujano E.; Franco, C. *Appl. Catal. A: General* **1993**, *100*, 85.
27. Thangaraj, A.; Kumar, R.; Mirajkar, P.; Ratnasamy, P., *J. Catal.* **1991**, *130*, 1.
28. Inui, T.; Matsuda, H.; Yamase, O.; Nagata, H.; Fukuda, K.; Ukawa, T.; Miyamoto, A. *J. Catal.* **1986**, *98*, 491.
29. Kumar, R.; Ratnasamy, P. *J. Catal.* **1990**, *121*, 89.
30. van der Pol, A.J.H.P.; Verduyn, A.J.; van Hoof, J.H.C. *Applied Catalysis A: General* **1992**, *92*, 113.
31. Bellucì, G.; Maddinelli, G.; Carati, A.; Gervasini, A.; Millini, R., in *Proceedings from the Ninth International Zeolite Conference*; von Ballmoos, R.; Higgins, J. B.; Treacy, M. M. Eds.; Butterworth-Heinemann: 1992; p 207.
32. Reference 31, p 155.
33. *Comprehensive Supramolecular Chemistry*; Atwood, J. L.; Davis, J. E. D.; Vögtle, F. Eds.; Pergamon: 1996; Vol. 7, p 430.